BUCKLING OF TWO-PHASE INHOMOGENEOUS COLUMNS AT ARBITRARY PHASE CONTRASTS AND VOLUME FRACTIONS

Mohammed G. Aldadah, Shivakumar I. Ranganathan and Farid H. Abed

msp

mmsp

BUCKLING OF TWO-PHASE INHOMOGENEOUS COLUMNS AT ARBITRARY PHASE CONTRASTS AND VOLUME FRACTIONS

MOHAMMED G. ALDADAH, SHIVAKUMAR I. RANGANATHAN AND FARID H. ABED

Buckling is an instability encountered in a wide variety of problems, both in engineering and biology. Almost all engineering structures are designed with adequate safety factors to prevent failure due to buckling, yielding or dynamic loads. In a classical sense, design for buckling is done by carefully controlling the modulus of elasticity, moment of inertia and the length of the structure. Further, such an approach assumes the material to be homogeneous and does not generally account for the microstructural details of the column. In this paper, we study the buckling of inhomogeneous columns with a two-phase checkerboard microstructure. Monte Carlo simulations are used to generate microstructures with arbitrary volume fractions and phase contrasts (ratio of the modulus of individual phases). An analytical form is obtained for the ensemble averaged critical buckling load based on the results of over 18,000 eigenvalue problems at arbitrary volume fractions, phase contrasts and distributions. Further, microstructural realizations that correspond to the highest buckling load (best design) and the lowest buckling load (worst design) are identified and the corresponding distribution of individual phases is determined. Finally, the statistical nature of the critical buckling load is discussed by computing the statistical moments that include the mean and coefficient of variation.

1. Introduction

Buckling is an instability phenomenon that leads to failure of slender members typically subjected to compressive loads. Perhaps the most widely used criterion for the buckling instability is Euler's buckling solution, which predicts the maximum axial compressive load that a slender, homogeneous and ideal column can carry. This classical result states that the critical buckling load is directly proportional to the modulus of elasticity, area moment of inertia, boundary conditions, and is inversely proportional to the square of the column length. This result is limited to long columns and does not account for material inhomogeneity. In reality, inhomogeneous materials are ubiquitous in nature and most materials exhibit inhomogeneity when the microstructural details are taken into account. Such materials can also be engineered to design columns with performance better than their homogeneous counterparts (for instance using 3D printing to create a functionally graded microstructure). Thus, there is an inherent need to understand the effect of material inhomogeneity on the overall response of such columns.

Although the buckling of inhomogeneous and functionally graded columns is still an ongoing area of research, there have been a few important studies that are noteworthy. Elishakoff and Rollot [1999] investigated columns with variable stiffness. In their study, Euler's buckling equation was modified to allow for variable stiffness across the length of the material. Then, using a preselected variable stiffness, the modified Euler equation was solved to obtain the critical buckling load. As a continuation of their

---

study, Elishakoff [2001] posed the same problem as an inverse buckling problem. The inverse method determined the stiffness distribution $k(x)$ and the critical buckling load P for a nonuniform beam with specified boundary conditions by using a preselected function for the buckling mode. Such a method produces results for a certain class of inhomogeneous materials, yet does not provide exact solutions for general heterogeneity.

Li [2001] derived a solution for the buckling load of nonuniform columns subjected to concentrated axial and distributed loads. In this approach, the governing equations were initially reduced using functional transformation and later solved using Bessel functions. The analytical solution provided results for twelve different cases that are important in engineering applications, such as high-rise buildings subjected to distributed loads. In yet another study, Huang and Li [2012] presented an analytical approach to determine the critical buckling load of a nonuniform column with or without continuous elastic restraint. Their study identified an optimal ratio between the radius in the middle of the cylinder and the radius at the end for maximum carrying load capacity.

Altus et al. [2005] introduced a new method for obtaining the buckling load analytically for linear inhomogeneous materials using the functional perturbation method (FPM). According to them, this method provided more accurate results for linear inhomogeneous materials than the conventional Galerkin and Rayleigh–Ritz methods. Along similar lines, Huang and Luo [2011] derived a solution for the buckling of inhomogeneous beams by using power series to represent the mode shapes. The power series method used was illustrated by studying a composite beam under various end supports. In addition, Morimoto and Tanigawa [2006] investigated the buckling of inhomogeneous rectangular plates subjected to uniform in-plane shear. In their study, an inhomogeneity parameter was introduced which in turn contributed to the bending rigidity. Also, as the inhomogeneity parameter was increased, the buckling load increased, whereas the buckling mode shape was unaffected. Furthermore, Earls [2007] emphasized the numerical limitations of using finite element modeling and eigenvalues in the solution of buckling equations. The limitations included differing results for the same structures using different software packages, and the stability of the results. This indicated the necessity to carefully assist the finite element solution with closed form analytical solutions or experiments wherever possible.

More recently, Li et al. [2011] solved the buckling equation for composite nonuniform columns with distributed axial loads or tip forces and used the solution to tailor materials such that the ratio of the buckling load to the weight is maximized for axially graded inhomogeneous composite columns with uniform cross-section. The optimization technique was performed on a column with a clamped end and a free end and resulted in the need to increase material density around the free end to increase the maximum load carrying capacity. Also, Singh and Li [2009] formulated a transcendental eigenvalue problem for elastically restrained functionally graded columns. In the problem they approximated a nonhomogeneous column with a piecewise function with constant geometrical and material properties. The resulting eigenvalue problem was then solved using a new numerical algorithm with different boundary conditions.

This paper presents a new study investigating the buckling capacity of inhomogeneous columns with two-phase checkerboard microstructures at arbitrary phase contrasts and volume fractions. To the best of our knowledge, the buckling of such two-phase checkerboard columns has not been investigated in the past. The microstructure of this column is made up of two materials with very different elastic moduli. A Monte Carlo technique is used to generate checkerboard microstructures at arbitrary phase contrasts, volume fractions and spatial distributions of the phases. After generating the microstructure,

the eigenvalue problem is then solved numerically using linear perturbation analysis that is implemented in the commercial finite element software ABAQUS [2004]. This procedure is repeated for all microstructural realizations, with the following objectives: (i) determine the critical buckling load for checkerboard columns as a function of the volume fraction; (ii) study the effect of phase contrast on the critical buckling load; (iii) identify the microstructural realizations (spatial distribution of individual phases) that result in achieving the highest and the lowest buckling loads for a given volume fraction.

2. Problem formulation

2.1. *General buckling equation.* The governing equation for the buckling of an inhomogeneous long column is given by the equation

$$E(x)I\frac{\partial^2 v}{\partial^2 x} + P_{\text{cr}}v = 0, \tag{1}$$

where $E(x)$ indicates the spatial dependence of the modulus of elasticity, I represents the area moment of inertia, v is the transverse deflection and P_{cr} is the critical buckling load. It is well-known that for a homogeneous column with $E(x) = E$, the critical buckling load is given by $P_{\text{cr}} = C\pi^2 EI/L^2$. Here, C is a constant representing the type of boundary condition and L is the column length.

In the present study, the microstructure is a two-phase material with a random checkerboard microstructure. Such a random checkerboard can be considered as a set of deterministic checkerboards: $\text{B} = \{B(\omega) : \omega \in \Omega\}$ (see [Ostoja-Starzewski 1998]). Here, Ω is the realization space ($\Omega = 2^{100}$) and ω is the specific microstructural realization under consideration. For a two-phase checkerboard column with phases 1 and 2, $B(\omega) = B_1 \cup B_2$, with the local moduli of elasticity given by E_1 and E_2, respectively. Mathematically, the microstructure can be defined completely using the indicator function defined as [Ostoja-Starzewski 1998]

$$\chi_1(\vec{x}, \omega) = \begin{cases} 1 & \text{if } \vec{x} \in B_1, \\ 0 & \text{if } \vec{x} \in B_2. \end{cases} \tag{2}$$

Using (2), the local modulus of elasticity at any point in the column can be identified as follows:

$$E(\vec{x}, \omega) = \chi_1(\vec{x}, \omega)E_1 + [1 - \chi_1(\vec{x}, \omega)]E_2, \tag{3}$$

where $\vec{x}$ is a position vector and E_1 and E_2 are the moduli of elasticity of the individual phases. The volume fraction of phase 1 can be simply recovered by the ensemble averaging of the indicator function

$$\alpha = \langle \chi_1 \rangle. \tag{4}$$

Due to the randomness introduced in the distribution of the individual phases as well as the volume fraction, it is difficult to find an analytical solution to (1) that simultaneously satisfies continuity of displacement and tractions between the individual phases. Thus, in this study we use Monte Carlo runs along with finite element analysis to solve (1) and obtain the critical buckling load for each realization.

2.2. *Finite element modeling using linear perturbation analysis.* As mentioned previously, a Monte Carlo technique is employed to generate checkerboard microstructures at arbitrary phase contrasts, volume fractions and the spatial distributions of the phases. After generating the microstructure, the eigenvalue problem is then solved numerically using linear perturbation analysis using the finite element
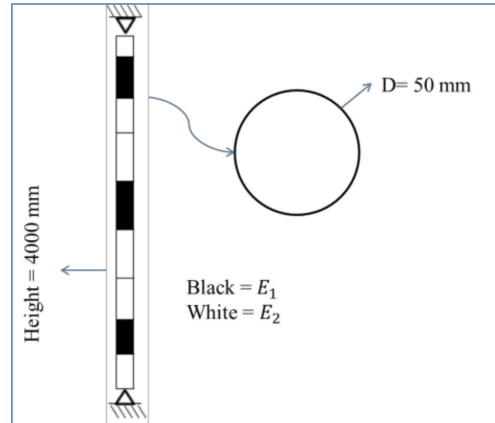
Figure 1. Two-phase checkerboard column with circular cross section.

software ABAQUS due to its versatility in handling such problems. A linear perturbation analysis step provides the linear response of the system about the base state, and estimates elastic buckling load via eigenvalue extraction. Eigenvalue buckling is generally used to approximate the critical buckling loads of stiff structures. Usually the loading on stiff structures is either an axial or membrane loading. The response to such loading involves small deformation before buckling. A simple example of stiff structure is the Euler column, which responds very stiffly to a compressive axial load until a critical load is reached, when it bends suddenly and exhibits a much lower stiffness. However, estimation using general eigenvalue extraction is useful, especially if the perturbation loads are elastic before the buckling occurs. The eigenvalue solution is obtained by making the model stiffness matrix singular. The model matrix is then described by $K^{ij}v^i = 0$, where K^{ij} is the tangent stiffness matrix and v^i is the displacement matrix [ABAQUS 2004].

In the proposed study, a column with a circular cross-section with diameter 50 mm and length of 4000 mm was used for the proposed analysis (see Figure 1). The dimensions were chosen such that elastic buckling is always ensured. Pinned connections were considered for both ends. The column is modeled with different material configurations for each simulation using deformable Timoshenko beam elements coded as B21 in ABAQUS. This type of line element accounts for the transverse shear stress. This is because Schnabl and Planinc [2011] have demonstrated that the transverse shear stress does affect the critical buckling load. Also, the B21 element is of much relevance to the current study as it provides better results for slender beams [ABAQUS 2004]. As for the boundary condition used in the FE modeling, the pin-pin connection was modeled by not allowing deformation in the axial and transverse directions for the bottom end. The restriction of deformation was only applied on the transverse direction for the top end to allow loading in the axial direction.

2.3. *Materials combinations.* In each analysis step, the column consists of two materials with different elastic modulus (E). The choice of the two materials used is based on the contrast, which is the ratio between the largest and the smallest elastic moduli, and can be calculated using the equation

$$k = E_1/E_2. \tag{5}$$

Material 1	Material 2	E_1 (GPa)	E_2 (GPa)	k
Steel	Magnesium	200	45	4.44
Steel	Wood	200	11	18.2
Magnesium	Wood	45	11	4.1
Copper	Aluminum	168	69	2.43

Table 1. Material combinations.

Table 1 presents the material combinations considered in the present study. The choice of materials was purely on the basis of providing different levels of contrast varying from very low to very high ratios. Columns made of steel and wood have the highest contrast, while columns made of aluminum and copper hold the lowest contrast. The other two conditions have almost equal contrasts. The use of a similar contrast helps in identifying behavioral similarities of the material combinations.

3. Methodology

For each analysis realization, the column is discretized into 100 segments, and each segment is assigned a random combination of E_1 and E_2. The volume fraction is changed by increasing the fraction of E_1 from 0% to 100% in increments of 10%. For each value of the E_1 volume fraction (10%, ..., 90%), the numerical simulations are performed 500 times to account for material randomness; moreover, the simulations are repeated for each material combination, with values of contrast k equal to, respectively, 2.43, 4.1, 4.4 and 18.2. Thus a total of $9 \times 4 \times 500 = 18{,}000$ runs were conducted, in order to determine the critical buckling load and to identify the microstructural realizations (spatial distribution of individual phases) that resulted in the highest and the lowest buckling loads for each volume fraction.

Figure 2 highlights the methodology employed in the current study. In step (a), a particular realization of the checkerboard is sampled randomly and its finite element model is set up in ABAQUS. The pin-pin
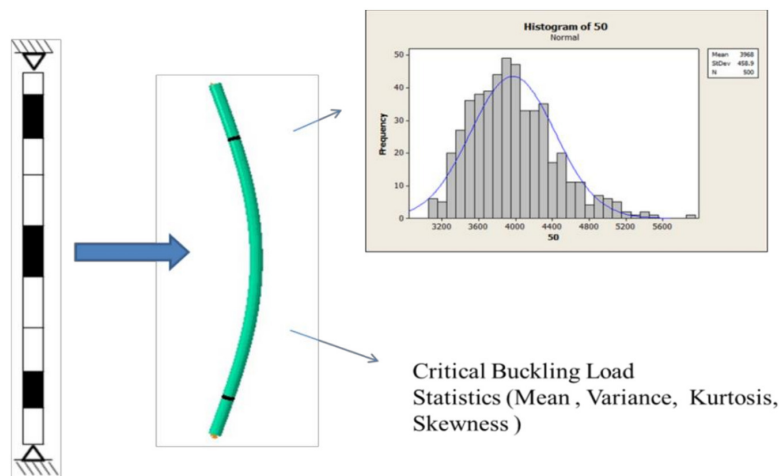

Figure 2. Methodology employed: microstructure of the column (left), buckling mode shape (middle), and statistical moments (right).

boundary conditions are then applied at the column ends. Next, in step (b), a concentrated unit load was applied and the eigenvalue problem was solved to obtain the mode-one critical buckling load and the corresponding mode shape. The procedure was repeated over 18,000 times in order to cover the entire realization space.

Subsequently, in step (c), the results were compiled to determine the minimum, maximum and ensemble averaged buckling load for each volume fraction and contrast. Also, the spatial distributions of the phases corresponding to the maximum and minimum buckling load were determined to identify the microstructure that corresponds to the best and worst designs, respectively. Finally, statistical analysis of the results was performed to obtain various statistical moments such as the mean and coefficient of variation.

4. Results and discussion

4.1. *Critical buckling load of the checkerboard column as a function of the volume fraction.* Prior to a discussion on the numerical results, it is convenient to define a rescaled buckling load, as follows:

$$P_c = \frac{P_{cr}L^2}{\pi^2 I},\tag{6}$$

where P_{cr} is the numerically obtained mode-one critical buckling load and P_c is the rescaled buckling load (typically in GPa). An alternative interpretation of P_c would be the equivalent effective elastic modulus of the checkerboard column. Depending upon the context, P_c could either represent the mean, minimum or the maximum rescaled buckling load.

Figure 3, left, presents the rescaled buckling load (average, maximum and minimum) for a checkerboard column made up of steel and wood. The modulus of elasticity for wood is 11 GPa and that of steel is 200 GPa, and thereby the contrast of the microstructure is $k = 18.2$. It is evident from this figure that the lower-modulus material (wood) affects the rescaled buckling load significantly more than the material with higher modulus (steel). Even at 50% volume fraction, the average value of the rescaled buckling load is only about 20.85 GPa. Similarly, the rescaled buckling load (average, maximum and
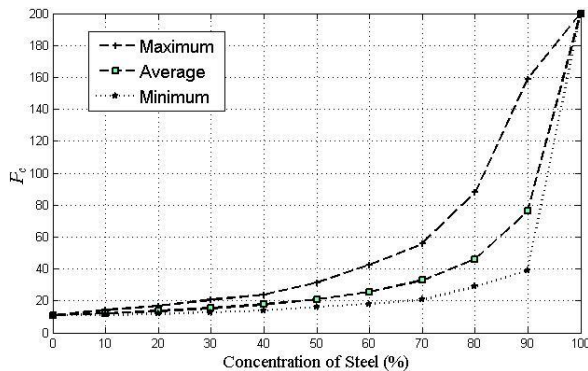
steel and wood microstructure ($k = 18.2$)   steel and magnesium microstructure ($k = 4.44$)
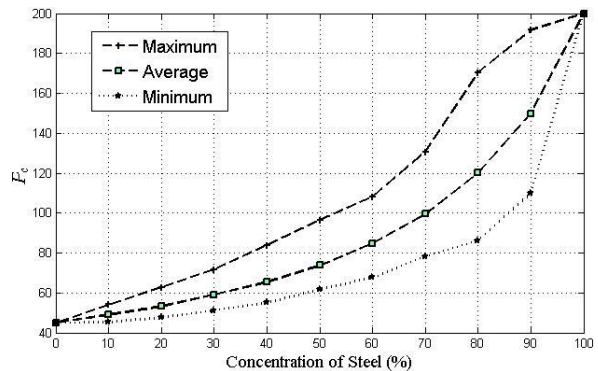
Figure 3. Rescaled buckling load (average, maximum and minimum) as a function of the volume fraction, for the first two material combinations.

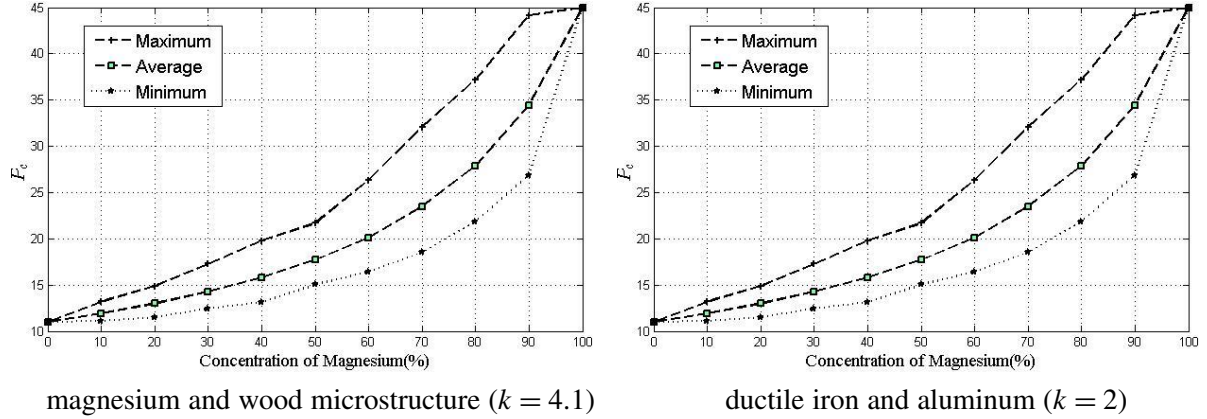magnesium and wood microstructure ($k = 4.1$)   ductile iron and aluminum ($k = 2$)

Figure 4. Rescaled buckling load (average, maximum and minimum) as a function of the volume fraction, for the last two material combinations.

minimum) for checkerboard columns made up of steel and magnesium ($k = 4.44$) and magnesium and wood ($k = 4.1$) are plotted in Figure 3, right, and Figure 4, left. The material properties for the individual phase are given in Table 1. It is evident from these plots that as the volume fraction of the stiffer material increases, the rescaled buckling capacity of the column increases. At a volume fraction of 50%, the rescaled buckling loads are 73.46 GPa and 17.68 GPa, respectively. Further, it can be noticed that the trends for the average, minimum and maximum rescaled buckling loads are identical for microstructures with similar contrasts. Finally, the rescaled buckling load (average, minimum and maximum) for ductile iron and aluminum is plotted in Figure 4, right. This particular microstructure has a contrast of 2.43.

Based on the numerical results obtained, it is possible to infer the analytical form for the average value of the rescaled buckling load as well as the ensemble averaged critical buckling load, as given in the equations

$$\langle P_c \rangle = \frac{E_1 E_2}{\alpha E_2 + (1 - \alpha) E_1} \qquad \text{(rescaled ensemble averaged buckling load)}, \qquad (7a)$$

$$\langle P_{cr} \rangle = \frac{\pi^2 I}{L^2} \frac{E_1 E_2}{\alpha E_2 + (1 - \alpha) E_1} \qquad \text{(ensemble averaged buckling load)}. \qquad (7b)$$

Here, E_1 and E_2 are the individual phase elastic moduli, α is the volume fraction of the phase 1, and the operator $\langle \cdot \rangle$ indicates the ensemble averaging.

4.2. *Effect of phase contrast on critical buckling load.* In order to clearly understand the effect of phase contrast, the notion of normalized buckling load is introduced. This is obtained by normalizing the maximum and minimum buckling load for each material combination with the ensemble averaged buckling load for the given combination:

$$P_n = P_{cr} / \langle P_{cr} \rangle. \qquad (8)$$

In Figure 5, left, the normalized buckling load is plotted as a function of contrast and volume fraction of the stiffer phase. When the volume fraction is 0% or 100%, all the curves converge to $P_n = 1$. This is
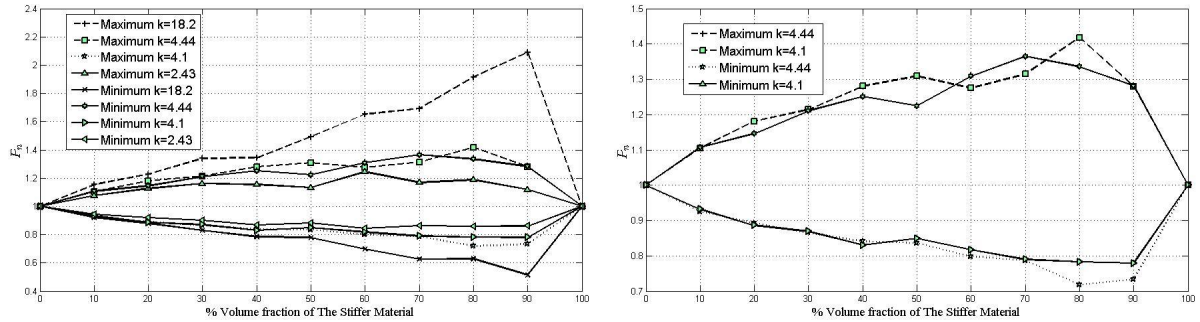
Figure 5. Normalized buckling load (maximum and minimum) as a function of the volume fraction of the stiffer phase. Left: differing contrasts. Right: similar contrasts.

because the microstructure is essentially homogeneous at these volume fractions. It is also evident from this plot that with increasing contrast, the curves for maximum and minimum normalized buckling loads are farther apart. Furthermore, from Figure 5, right, it is evident that these curves are identical when the contrasts are similar. Based on these observations, one can postulate the following functional form for the normalized buckling load:

$$P_n = f(\alpha, k). \tag{9}$$

4.3. *Spatial distribution of individual phases.* In order to determine the spatial distribution of individual phases corresponding to the maximum (best column design) and minimum (worst column design) buckling loads, the corresponding buckling mode shapes are plotted as a function of volume fraction, as shown in Figure 6. The top panel corresponds to a contrast of 2.43 and the bottom one to a contrast of 18.2. From these graphs, it is evident that for maximizing the buckling load, it is desirable to distribute
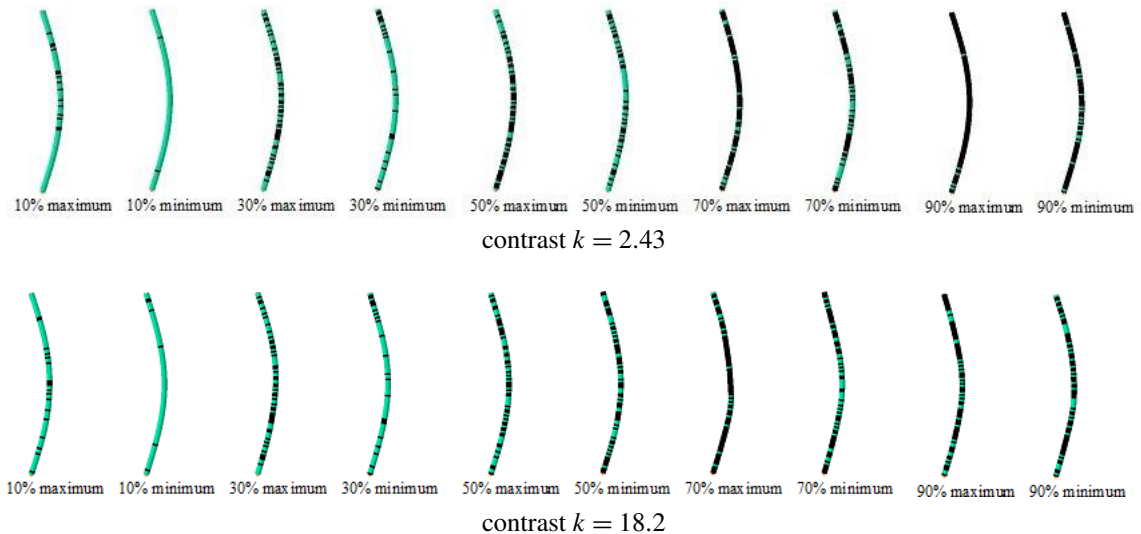
Figure 6. Buckling mode shapes corresponding to the maximum and minimum buckling load as a function of volume fraction.
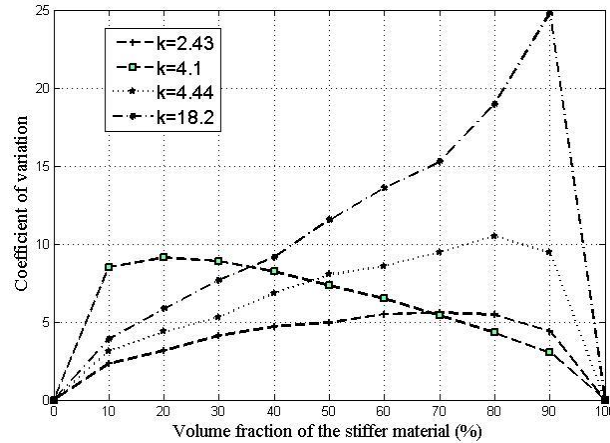
Figure 7. Data statistics: coefficient of variation.

the phase with higher stiffness in the middle of the column and vice versa for the minimum buckling load. This essentially implies that by allocating the phase with higher stiffness in the region with higher deflection, the buckling capacity is enhanced.

4.4. *Statistical analysis.* The numerical simulations performed in this study resulted in 18,000 simulations, and the pool of results for the buckling load is best analyzed using statistical tools that include the mean and coefficient of variation. The result on the mean value of the buckling load has been extensively discussed in the previous sections. The coefficient of variation for the data set is plotted as a function of contrast and volume fraction in Figure 7. As expected, it is zero for a homogeneous material that corresponds to 0% or 100% volume fraction. In general, as the contrast increases, the coefficient of variation also increases. It is interesting to note that the coefficient of variation for the steel-magnesium checkerboard ($k = 4.44$) and that of the magnesium-wood microstructure ($k = 4.1$) are about the same when the magnesium volume fraction is kept the same. Finally, it is worthwhile to note that the determination of higher moments such as the skewness and kurtosis would require significantly more realizations and would be computationally very expensive.

5. Conclusion

In this paper, a Monte Carlo technique was used to generate checkerboard microstructures at arbitrary phase contrasts, volume fractions and spatial distributions of the phases. Subsequently, the resulting eigenvalue problems were solved numerically in ABAQUS using linear perturbation analysis. The maximum, average and the minimum values for the critical buckling load were determined and the corresponding buckling mode shapes were identified under pin-pin boundary conditions. It was demonstrated that the ensemble averaged rescaled buckling load $\langle P_c \rangle$ was simply the volume-fraction weighted harmonic mean of the individual phase elastic moduli. Also, the normalized buckling load P_n was identical for microstructures with similar contrasts. Furthermore, it was demonstrated that distributing the phase with higher stiffness in regions of higher deflections (middle) maximizes the buckling capacity of the column and vice versa. Finally, a statistical analysis on the numerical results was conducted by studying the mean

and coefficient of variation as a function of contrast and volume fraction. To the best of our knowledge, this is the first time an analytical result has been proposed for the critical buckling load of a column with a random checkerboard microstructure.

References

[ABAQUS 2004] ABAQUS, *User manual 6.3*, Habbitt, Karlsson and Sorensen, Providence, RI, 2004.

[Altus et al. 2005] E. Altus, A. Proskura, and S. Givli, "A new functional perturbation method for linear non-homogeneous materials", *Int. J. Solids Struct.* **42**:5–6 (2005), 1577–1595.

[Earls 2007] C. J. Earls, "Observations on eigenvalue buckling analysis within a finite element context", in *Proceedings of the SSRC annual stability conference* (New Orleans, LA), edited by C. Stratman, Structural Stability Research Council, Rolla, MO, 2007.

[Elishakoff 2001] I. Elishakoff, "Inverse buckling problem for inhomogeneous columns", *Int. J. Solids Struct.* **38**:3 (2001), 457–464.

[Elishakoff and Rollot 1999] I. Elishakoff and O. Rollot, "New closed-form solutions for buckling of a variable stiffness column by Mathematica", *J. Sound Vib.* **224**:1 (1999), 172–182.

[Huang and Li 2012] Y. Huang and X.-F. Li, "An analytic approach for exactly determining critical loads of buckling of nonuniform columns", *Int. J. Struct. Stab. Dyn.* **12**:4 (2012), 1250027.

[Huang and Luo 2011] Y. Huang and Q.-Z. Luo, "A simple method to determine the critical buckling loads for axially inhomogeneous beams with elastic restraint", *Comput. Math. Appl.* **61**:9 (2011), 2510–2517.

[Li 2001] Q. S. Li, "Exact solutions for buckling of non-uniform columns under axial concentrated and distributed loading", *Eur. J. Mech. A Solids* **20**:3 (2001), 485–500.

[Li et al. 2011] X.-F. Li, L.-Y. Xi, and Y. Huang, "Stability analysis of composite columns and parameter optimization against buckling", *Compos. B Eng.* **42**:6 (2011), 1337–1345.

[Morimoto and Tanigawa 2006] T. Morimoto and Y. Tanigawa, "Linear buckling analysis of orthotropic inhomogeneous rectangular plates under uniform in-plane compression", *Acta Mech.* **187**:1-4 (2006), 219–229.

[Ostoja-Starzewski 1998] M. Ostoja-Starzewski, "Random field models of heterogeneous materials", *Int. J. Solids Struct.* **35**:19 (1998), 2429–2455.

[Schnabl and Planinc 2011] S. Schnabl and I. Planinc, "The effect of transverse shear deformation on the buckling of two-layer composite columns with interlayer slip", *Int. J. Non-Linear Mech.* **46**:3 (2011), 543–553.

[Singh and Li 2009] K. V. Singh and G. Li, "Buckling of functionally graded and elastically restrained non-uniform columns", *Compos. B Eng.* **40**:5 (2009), 393–403.

MOHAMMED G. ALDADAH: maldadah@alumni.aus.edu
Department of Mechanical Engineering, American University of Sharjah, 26666, United Arab Emirates

SHIVAKUMAR I. RANGANATHAN: ranganathan@rowan.edu
Department of Mechanical Engineering, Rowan University, 201 Mullica Hill Road, Glassboro, NJ 08028, United States

FARID H. ABED: fabed@aus.edu
Department of Civil Engineering, American University of Sharjah, 26666, United Arab Emirates

JOURNAL OF MECHANICS OF MATERIALS AND STRUCTURES

msp.org/jomms

Founded by Charles R. Steele and Marie-Louise Steele

Cover photo: Wikimedia Commons